JOURNAL OF GUIDANCE, CONTROL, AND DYNAMICS
Vol. 15, No. 3, May-June 1992

Robust Modal Identification/Estimation of the Mini-Mast Testbed

Michael J. Roemer*
Lord Corporation, Erie, Pennsylvania 16514
and
D. Joseph Mook†
State University of New York at Buffalo, Buffalo, New York 14260

The Mini-Mast is a 20-m-long, three-dimensional, deployable/retractable truss structure designed to imitate future trusses in space. This structure has undergone various static and dynamic experiments to identify its modal properties so that control laws can be developed and tested. This paper presents results from a robust (with respect to measurement noise sensitivity), time-domain, modal identification technique for identifying the modal properties of the Mini-Mast structure even in the presence of noisy measurements. Three testing/analysis procedures are considered: 1) sinusoidal excitation near the resonant frequencies of the Mini-Mast, 2) frequency response function averaging of several modal tests, and 3) random input excitation with a free response period. The results indicate that the robust technique of the paper is more accurate using the actual experimental data than are existing techniques.

Introduction

RECENTLY, many experimental modal analysis (EMA) techniques have been developed to improve current modal testing and analysis procedures. Modal analysis techniques can usually be classified as either frequency or time-domain procedures. Some experimental difficulties arise in the frequency domain when the natural frequencies of a system are closely distributed and/or the system contains a high degree of damping. In the time domain, noisy output measurements are the most troublesome for accurate modal identification. However, both time and frequency domain methods encounter the most difficulty when particular modes are poorly excited during a testing procedure. For this case, the amplitudes of the poorly excited modes can be less than the root mean square (RMS) amplitude of the noise. In this paper, a time-domain identification algorithm that is robust with respect to measurement noise is used to identify some of the primary modes of the Mini-Mast testbed at the NASA Langley Research Center.

The modal identification algorithm used in this paper combines the eigensystem realization algorithm (ERA) identification/realization technique[1] with an optimal state estimation algorithm called minimum model error[2] (MME) to identify modal properties of a structure successfully even in the presence of noisy measurements. The ERA technique is based on the singular value decomposition of a generalized Hankel matrix composed of discrete, time-domain measurements. This time-domain technique is capable of accurately identifying modal parameters for cases involving perfect or low-noise measurements. However, difficulties may arise when high noise levels are present in the output measurements. Thus, by combining the MME optimal state estimation algorithm with the ERA identification algorithm, improved modal identification is achieved through lowering the sensitivity to noise. This ability has been demonstrated in numerous simulations of different test systems.[3-6]

Received July 2, 1990; revision received May 9, 1991; accepted for publication July 1, 1991. Copyright © 1992 by the American Institute of Aeronautics and Astronautics, Inc. All rights reserved.

*Engineering Specialist. Member AIAA.
†Associate Professor, Department of Mechanical and Aerospace Engineering. Senior Member AIAA.

The MME estimation algorithm is well suited for the modal identification problem because it does not assume that the model error is a white noise of known covariance as do other estimation filters (e.g., Kalman filter). Instead, the model error is assumed to be an unknown quantity and is estimated as part of the solution. The theoretical advantages of this assumption are obvious for the present problem, since the model is unknown a priori. Since the model is composed of deterministic modes, the identification problem is one of finding (eliminating) deterministic model error. In several previous studies, the MME has been shown to produce state estimates of high accuracy for problems involving both significant model error and significant measurement error.[7]

Using the MME procedure to reduce the noise sensitivity of the ERA has been investigated in several computer simulations. The results were obtained on three and four mode simulated truths to which Gaussian distributed white noise was added to simulate noisy measurements. The ERA was found to be extremely accurate at low noise levels. However, the accuracy is diminished if the measurement noise is increased enough to affect the lower amplitude modes. This result was also reported by Juang and Pappa.[8] However, compared with ERA by itself, the combined ERA/MME algorithm produced more accurate results with respect to identifying the number of modes, frequencies, damping ratios, and mode shapes. For example, in a four mode simulation example using noisy measurements with a noise level of 5% of the measurement amplitudes, the ERA algorithm could only identify three of the four modes. The combined ERA/MME algorithm, on the other hand, identified all four modes and their respective mode shapes accurately. The purpose of this paper is to extend this theoretical/simulation background to the Mini-Mast control structures interaction (CSI) testbed to examine its identification ability on actual experiment data taken from a large space structure.

Minimum Model Error Estimation

The MME estimation procedure, formulated in state space, combines an assumed model with discrete measurements to obtain optimal estimates of the state trajectories of a dynamic system. The assumed model is constructed using whatever information and insight the modeler may have. In this application, the assumed model is the realized model identified by the ERA. The MME estimation presupposes that the assumed

model is imperfect, and model correction terms are included in the formulation. The MME then processes the available measurements in conjunction with the model to determine estimates of both the state trajectories and model error.

A typical postexperiment state estimation problem may be stated as follows: Given a system whose state vector dynamics are modeled by the linear or nonlinear system of equations

$$\dot{x} = f[x(t),u(t),t] \tag{1}$$

where x is the $n \times 1$ state vector, f the $n \times 1$ vector of model equations, u the $p \times 1$ vector of forcing terms, and the set of discrete measurements are given as

$$\tilde{y}(t_j) = g_j\{[x(t_j),t_j]\} + v_j \tag{2}$$

where $y(t)$ is the $r \times 1$ measurement set at time t_j, g the $r \times 1$ measurement model equations, m the number of measurement sets, and v_j the $r \times 1$ measurement error vector, that determines the optimal estimate for $x(t)$ during a specified time interval.

Rather than implementing the usual approach of minimizing a function of the estimate error covariance, the MME's optimal state trajectory estimate is determined on the basis of the assumption that the measurement-minus-estimate error covariance matrix must match the measurement-minus-truth error covariance matrix. This condition is referred to as the "covariance constraint." The covariance constraint is defined mathematically by requiring the following approximation to be satisfied:

$$R_J \approx \left(\{\tilde{y}(t_j) - g[\hat{x}(t_j),t_j]\}\{\tilde{y}(t_j) - g[\hat{x}(t_j),t_j]\}^T \right) \tag{3}$$

Thus, the estimated measurements $g[\hat{x}(t_j,t_j)]$ are required to fit the actual measurements with approximately the same error covariance as the actual measurements fit the truth. Otherwise, the estimate cannot be correct. Once the covariance constraint has been satisfied, the state estimate is considered to have been optimized.

A significant advantage of the MME is that no assumption of the model error covariance is needed. Model error is represented by adding a to-be-determined unmodeled disturbance vector $d(t)$ to the right side of the original state model equations:

$$\dot{x} = f[x(t),u(t),t] + d(t) \tag{4}$$

In the MME formulation, Eqs. 1–4 are used with the following cost function that is minimized with respect to $d(t)$:

$$J = \sum_{j=1}^{m} \left(\{\tilde{y}(t_j) - g[\hat{x}(t_j),t_j]\}^T R_j^{-1} \{\tilde{y}(t_j) - g[\hat{x}(t_j),t_j]\} \right) + \int_{t_0}^{t_f} d(\tau)^T W d(\tau)\, d\tau \tag{5}$$

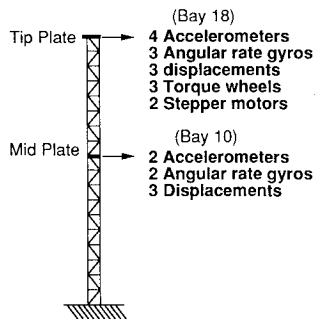

Fig. 1 NASA mini-mast testbed.

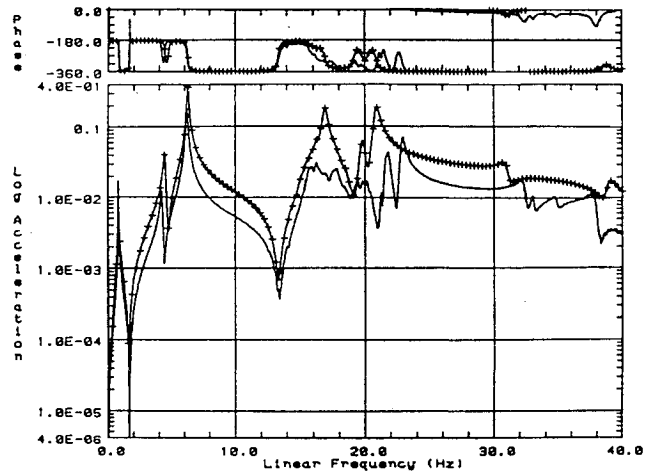

Fig. 2 Mini-Mast frequency response function.

where W is a to-be-determined weight matrix. This set of equations is mathematically similar to the classical optimal control problem, and consequently an associated two-point boundary value problem (TPBVP) must be solved.[9] The weighting R_J on each of the discrete penalty terms is the associated measurement error covariance matrix, and the W is found so that the covariance constraint is satisfied. The solution of the MME yields an optimal estimate for $x(t)$, which may then be used as "new measurements" for a time-domain identification scheme. In the next section, we combine the MME with the ERA to produce a less noise-sensitive algorithm for identifying the modal properties of the Mini-Mast testbed.

Mini-Mast Testing Procedure

The Mini-Mast is a deployable/retractable test truss structure designed to imitate future trusses to be used in space. A representative illustration supplied by NASA is shown in Fig. 1. The Mini-Mast is approximately 20 m in length (18 bays, 1.12 m each) and has a three-longeron construction forming a triangular cross section with points inscribed by a circle of 1.4 m in diameter.[10] The truss is cantilevered vertically to the ground by bolting the lowest three joints. The joints are made of machined titanium (6A1-4V) to hinge the longeron and diagonal members securely. The tubing members are constructed of a graphite/epoxy composite. The Mini-Mast has undergone various static and dynamic experiments. The work of this paper is concentrated on the data taken from selected dynamic tests.

Several types of response sensors are available on the Mini-Mast testbed. The sensors chosen for the dynamic tests discussed here are Kaman KD-2300 displacement probes. The probes are positioned to measure deflections orthogonal to the face of the probe and are mounted parallel to the Mini-Mast's corner joints. All of the bays except bay 1 are instrumented with three of these displacement sensors. The operating principle of the sensors is based on the impedance variations caused by eddy currents induced in a conductive metal target. The displacement is sensed from the coupling between a coil in the sensor and a particular target. Resolution of the Kaman KD-2300-10CU at midrange is 0.0025 mm with a static frequency response up to 50 kHz.

Three testing/analysis procedures are examined. First, frequency response functions (FRF) were constructed from 1) a finite element model and 2) experimental data supplied by NASA's Spacecraft Dynamics Branch. A plot illustrating the type of data used in this analysis is shown in Fig. 2.

Referring to Fig. 2, the FRF distinguished by the crosses represents the finite element or analytical model. The other FRF is derived from many sets of experimental data and

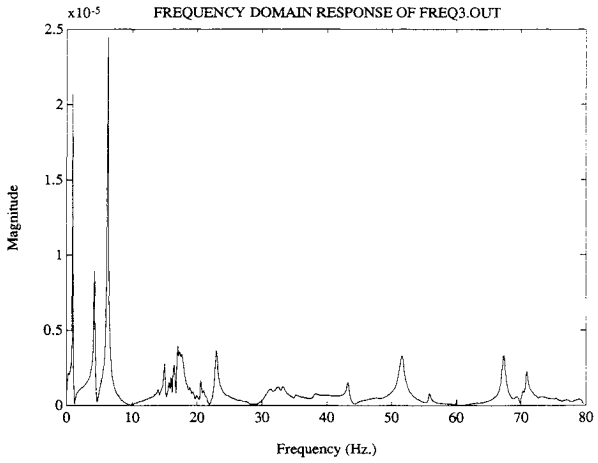

Fig. 3 Frequency response.

generated using Structural Dynamics Research Corporation's (SDRC) I-DEAS test analysis package. The first analysis procedure discussed in this paper identifies the modal properties of the Mini-Mast structure by taking inverse Fourier transforms of the averaged FRFs and using them as input to the identification algorithm. The identified natural frequencies establish a "truth" for comparing the other identification and testing procedures. The second testing procedure consisted of exciting the Mini-Mast test structure at frequencies close to its predicted natural frequencies. The time domain responses are then transformed into the frequency domain where a transfer function is formulated using auto and cross correlations. Finally, the impulse response (to be analyzed) is found by transforming back to the time domain. The third testing/analysis procedure consisted of randomly exciting the Mini-Mast structure and then allowing it to free decay until it comes to rest. Two response points were monitored at bay 10 at a sampling rate of 128 Hz. The response portion used in the identification/estimation algorithm included 100 data points from the free response of the structure. The combined ERA/MME algorithm was compared against the ERA by itself. The results were compared with respect to the following criteria: 1) the truth established by the frequency response function averaging, 2) damping ratio identification, and 3) modal amplitude coherence factors. Improvements were noted with respect to all three performance measures.

Frequency Response Function Analysis

The inverse Fourier transforms of selected FRFs were obtained to get a representative impulse time history. This impulse response data was then filtered so that a small frequency bandwidth could be investigated closely.The first frequency bandwidth considered was 0–10 Hz. In this region, the first and second bending modes were observed as well as the first torsion mode. Included in the frequency range of 10–20 Hz are a cluster of 108 "local" modes. These modes are primarily due to the bending of the 54 diagonal truss members. The final frequency range considered was 20–30 Hz. In this range, the second torsion mode was identified. The transformed time-domain data were used as input to the combined ERA/MME algorithm. A summary of the steps asociated with this experimental analysis is provided below.

Modal Identification Algorithm

1) Obtain time-domain measurements from either the inverse transforms of the frequency response functions or raw data from the Mini-Mast.

2) Apply the ERA to the measurements obtained in step 1 to realize a model.

3) Input the realized model from step 2, along with the measurements, into the MME algorithm to produce optimal state estimates.

4) Sample the MME-produced state estimates at discrete-time intervals to create simulated measurements of higher accuracy than the original measurements.

5) Apply ERA to the simulated measurements to realize/identify the new modal parameters.

6) Examine the identified modal parameters for some convergence criteria, and repeat the procedure if necessary.

The first two bending and torsion modes of the Mini-Mast were isolated as modes of particular interest in this paper. Utilizing a 10th-order, Butterworth, low-pass filter, the first two bending modes and the first torsion mode were clearly identified using the FRF data. Because the exact frequencies of the Mini-Mast are unknown, a small range is given for each identified frequency to serve as the "truth". Using the Fourier inverse of several averaged data sets, the first bending mode frequency was identified in the range of 0.87–0.88 Hz, the first torsion mode frequency between 4.20–4.35 Hz, and the second bending mode frequency was in the range of 6.25–6.35 Hz. The second torsion mode frequency was identified with the help of a 10th-order, Butterworth, band-stop filter. A band-stop filter was chosen to filter out the effects of the 108 local modes in the frequency range of 10–20 Hz. The identified natural frequency of the second bending mode was between 22.1–22.7 Hz. An illustration of the frequency and time-domain equivalents used in this analysis are shown in Figs. 3 and 4. The FRF shown in Fig. 3 was data taken from the Mini-Mast averaged many times. The time-domain response of Fig. 4 was obtained directly from the inverse fast Fourier transform (FFT) of the frequency response data of Fig. 3.

The identification results presented earlier are produced from the combined ERA/MME algorithm. However, the ERA algorithm alone produced the same results. This result is expected because the frequency response functions were formed from an average of several tests. Also, the averaged FRFs were filtered to isolate the particular modes to be identified. This averaging/filtering used before identification essentially eliminated the noise content of the data. The ranges of the Mini-Mast's first four natural frequencies of interest are given as follows: $\omega_{b1} \approx 0.87$–0.88 Hz; $\omega_{t1} \approx 4.20$–4.35 Hz; $\omega_{b1} \approx 6.25$–6.35 Hz; and $\omega_{t1} \approx 22.1$–22.7 Hz.

Sinusoidal Excitation Analysis

In this section, the data used are obtained from sinusoidal excitations applied to the Mini-Mast test structure. The frequencies of the sinusoidal forces are set near the assumed natural frequencies of the structure in an attempt to produce a more accurate identification. A torque wheel located at the top of the mast was used to excite the structure, whereas the Kaman displacement probes sensed the structure's motion. Once the measurements from the input and output sensors are collected, a transfer function of the Mini-Mast can be con-

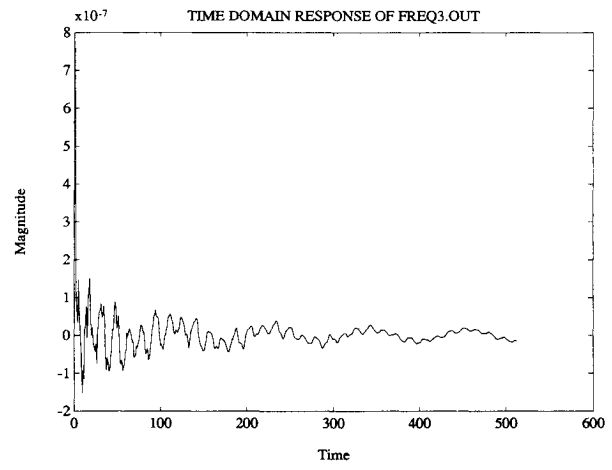

Fig. 4 Impulse response.

structed. The transfer function equation is composed of cross and auto correlations as follows:

$$G(jw) = S_{xx}(\omega)/S_{fx}(\omega) \tag{6}$$

where S_{xx} is the auto-spectral density, S_{fx} the cross-spectral density, and $G(jw)$ the frequency response or transfer function.

Equation (6) is based on the FFT of the input/output time histories. Excluding the initial transient response of the structure due to the torque wheel force, the frequency response is dominated by the frequency of excitation. A mathematical problem exists when computing the system's transfer function because at frequencies other than the excitation frequency, the Fourier transform of the input produces numbers very close to zero. Therefore, a problem of dividing by numbers that are very close to zero is unavoidable. To overcome this difficulty, a small amount of Gaussian distributed white noise with variance of 4×10^{-6} was added to the measurements. As expected, the addition of white noise produced larger numbers in the frequency response of this structure at frequencies other than the excitation frequency. After the transfer function is formulated, the impulse response can be generated for input to the identification algorithm. The impulse response is calculated by taking the inverse Fourier transform of the structure's transfer function or FRF.

The modal identification procedure starts by applying ERA on the impulse response data. Individual input/output time histories were used to construct a 100×100 Hankel matrix from which a model was realized. An average of five tests were used to arrive at the identified frequencies for both the ERA and ERA/MME algorithms. Most of the individual time histories only revealed information about a couple of the modes at one time. Therefore, several different time histories were used to obtain each identified natural frequency.

Following the step procedure of the ERA/MME algorithm, only two iterations were used for identifying the first four natural frequencies. Simple one- and two-mode models were used in the estimation/identification scheme. The use of these truncated models highlights the importance of not modeling the truncated modes as white noise. Table 1 illustrates all of the results.

Table 1 ERA and ERA/MME sine input results

	"Truth"	ERA	ERA/MME
	Frequency, Hz	Frequency, Hz	Frequency, Hz
One bending	0.87–0.88	0.8470	0.8668
One torsion	4.20–4.35	4.1175	4.4027
Two bending	6.25–6.35	7.0457	6.8943
Two torsion	22.1–22.7	22.150	22.091

Comparing the ERA and combined ERA/MME algorithms with the FRF analysis results indicates an overall improvement when using the combined procedure. More specifically, identification accuracy of the first three frequencies identified by the ERA/MME algorithm was improved by up to 5% over ERA by itself. The fourth frequency remained virtually the same.

In the preceding analysis, inverse and regular Fourier transformations were performed on the data to get the impulse time histories needed for time domain modal identification. Thus, the data were not raw time histories of response. The noise that might have been present in the original test data would have been altered significantly by these transformations. Therefore, the improvements in identification accuracy using MME estimation were not as significant as might be expected if raw impulse response data or data generated from random input excitations were used. This is shown in the next section.

Random Excitation/Free Response Analysis

In this section, the Mini-Mast test structure was excited using a random input with a bandwidth of 0–40 Hz. The random excitation was applied for 26 s, and then the structure was allowed to free respond until the response went to zero. Two response points were monitored at bay 10 of vortices A and B, and the shaker was located at bay 9. The data sampling rate was 128 Hz, and the free response portion of the time history began at the 33-s mark. The response portion that was used in the identification/estimation algorithm included 100 data points ranging in time from 34.0–34.8 s (the free response portion). The combined ERA/MME identification algorithm was compared against ERA by itself to examine the advantages of the combined technique. A predicated noise variance 1×10^{-12} (i.e., good measurements) was used in the MME estimation scheme to satisfy the covariance constraint.

The modal amplitude coherence (MAC) factors were calculated for each mode. MACs estimate the degree of modal excitation or controllability for each mode. A MAC factor close to 1 means that the mode was identified well during the testing procedure, whereas a MAC much less than 1 indicates the converse.

First, the identification results of the responses at bay 10, vortex A are shown in Tables 2 and 3. Improvements are found in the MAC factors for all four primary modes. However, a more distinct improvement was observed when identifying the two torsional modes. Specifically, the first torsional mode's MAC factor as identified by ERA was 0.8974, whereas the ERA/MME identified MAC factor was 0.9842. The MAC factor of the second torsional mode was identified by ERA as 0.8633, and the ERA/MME algorithm identified it as 0.9457. The improved MACs are also supported by the identified frequencies and damping ratios. The "true" torsional fre-

Table 2 ERA free response results

	"Truth"	ERA		
	Frequency, Hz	Frequency, Hz	Damping ratio	MACF, 0-1
One bending	0.87–0.88	0.8821	0.0377	0.9981
One torsion	4.20–4.35	4.7713	0.1019	0.8974
Two bending	6.25–6.35	6.1479	0.0287	0.9901
Two torsion	22.1–22.7	22.607	0.0322	0.8633

Table 3 ERA/MME free response results

	"Truth"	ERA/MME		
	Frequency, Hz	Frequency, Hz	Damping ratio	MACF, 0-1
One bending	0.87–0.88	0.8814	0.0240	0.9993
One torsion	4.20–4.35	4.3719	0.0044	0.9842
Two bending	6.25–6.35	6.2156	0.0299	0.9962
Two torsion	22.1–22.7	22.443	0.0164	0.9457

Table 4 ERA free response results (vortex B)

	"Truth"	ERA (b)		
	Frequency, Hz	Frequency, Hz	Damping ratio	MACF, 0-1
One bending	0.87-0.88	0.8585	0.1206	0.9914
One torsion	4.20-4.35	4.5576	0.0287	0.9546
Two bending	6.25-6.35	6.2174	0.0209	0.9925
Two torsion	22.1-22.7	22.324	0.0283	0.9472

Table 5 ERA/MME free response results (vortex B)

	"Truth"	ERA/MME (b)		
	Frequency, Hz	Frequency, Hz	Damping ratio	MACF, 0-1
One bending	0.87-0.88	0.8590	0.1217	0.9930
One torsion	4.20-4.35	4.3978	0.0072	0.9719
Two bending	6.25-6.35	6.2004	0.0211	0.9955
Two torsion	22.1-22.7	22.227	0.0272	0.9488

quencies were identified by the averaged FRFs in the range of 4.20-4.35 and 22.1-22.7 Hz. The torsional modes identified by ERA were 4.77 and 22.61 Hz, respectively, and those identified by the combined ERA/MME algorithm were 4.37 and 22.4 Hz, respectively, a supportive conclusion. The damping ratio of the first torsional mode identified by ERA was over 10%, and the ERA/MME technique identified it as 0.4%. Hence, when examining the MAC factors, natural frequencies, and damping ratios, the combined algorithm produced improved accuracy with respect to each one.

The identification results from the responses at bay 10, vortex B are given in Tables 4 and 5. The MAC factors for each identified mode are again improved. As in the preceding case, the most improved mode was the first torsional mode. The MAC factor identified by ERA was 0.9546, whereas the ERA/MME algorithm identified it as 0.9719. The natural frequency associated with this mode was identified by ERA to be 4.56 Hz, and the ERA/MME procedure identified it to be 4.39 Hz. Recall, the "true" natural frequency identified by the averaged FRFs was in the range of 4.20-4.35 Hz. The damping ratio was also reduced from 2.87% (using ERA) to 0.72% (using ERA/MME).

As shown in Tables 2-5, the MAC factors from the combined ERA/MME algorithm are indeed improved over the ERA for all four primary modes. The damping ratios were also seen to be improved, assuming that the damping ratios of the Mini-Mast are less than 5% (a reasonable assumption for such a structure). For example, the damping ratio of the first torsional mode identified by ERA was 0.101, and the ERA/MME identified it to be 0.0044. Note, the most improved damping ratios and MAC factors were found to be associated with the torsional modes of the Mini-Mast. This can be explained by the fact that the shaker was used in only one direction. Therefore, the linear or bending modes were excited more rigorously than the torsional modes.

This result highlights a major advantage of using the combined ERA/MME algorithm, namely, to help identify modes not excited very well in a testing procedure.

A further study was performed that focused on the assumptions of measurement error and concluded with the following important result. When predicting the measurement error covariances (the only input covariance needed for the ERA/MME algorithm), it is important to predict a low covariance in the beginning and slowly increase the prediction until the best modal amplitude coherence factors are found. The reason for this is that if the predicted measurement error covariance is lower than the unknown actual measurement error covariance, then the estimate can never be worse than the measurements are already. This result allows the user to trust the implementation of the ERA/MME algorithm. However, if the predicted measurement error covariance is higher than the unknown actual covariance, then the simulated measurements from the estimates could become worse (more noisy) than the original measurements. Because of this, it is important to assume measurement error covariances to be low when satisfying the covariance constraint of the MME estimation technique.

Conclusions

Data from three different modal testing techniques were used to compare ERA and ERA/MME algorithms for identifying some of the primary modes of NASA's Mini-Mast. The three techniques were FRF averaging, sinusoidal excitations, and impulse response analysis. The frequency response function analysis served to create a "truth" with which the sinusoidal excitation and impulse response tests could be compared. The authors believe the "truth" is accurate because of the many tests used to produce the averaged results.

The sinusoidal testing procedure included adding white noise to the original measurements so that a transfer function could be approximated. The transfer functions were then transformed into the time domain for input to the identification algorithms. Results from the identification algorithms revealed improvements (up to 5%) in identifying the first three natural frequencies of the Mini-Mast.

The third test included shaking the Mini-Mast structure with a random input for 26 s and then allowing the structure to come to rest. The results of this test gave the best improvements when compared with the other tests because the reduced sensitivity of the combined ERA/MME algorithm is most pronounced on raw impulse response or free response data. The other tests employed FFTs and inverse FFTs to construct the impulse responses, and these transformations essentially eliminate the presence of data noise. However, although FRFs and inverse FRFs eliminate noise, they do not necessarily give a good answer. Specifically, the results from the combined ERA/MME algorithm on raw data are more accurate than the results from ERA or ERA/MME on transformed data. This is probably the most important result of using the combined ERA/MME algorithm.

The identification of the torsional modes was especially improved using the combined identification/estimation algorithm. The identification improvements were based on 1) the damped natural frequencies identified by ERA/MME being closer to the FRF averaged identified frequencies than ERA alone, 2) the damping ratio identification, specifically having damping ratios approximately 2% or less, and 3) the modal amplitude coherence (MAC) factors being much closer to 1 than ERA alone. The most improved case was found in the identification of the first torsion mode. The ERA identified MAC factor was 0.8984, and the combined ERA/MME improved the MAC factor to 0.9842. Also, the damping ratio of this mode was identified by ERA to be 0.1019, and the ERA/MME identified it to be 0.0044, a noticeable improvement if the damping is indeed close to 0.

The fact that the MAC factors of the torsional modes were lower than the bending modes (for both the ERA and ERA/MME identification techniques) allows us to conclude that the torsional modes were not excited very well during the modal test. This concern, along with the improvements in the identification of the damping ratios and natural frequencies, was addressed by the ERA/MME identification scheme (specifically by the results of the free decay tests given in Tables 2–5). Hence, the combined identification/estimation algorithm can improve the time-domain identification methods in the case of noisy output measurements or poorly excited modes.

Acknowledgments

This work was supported by the NASA Langley Research Center under Contract NAG 1950. The data supplied for this paper were taken by Jeffrey L. Sulla of Lockheed and the Mini-Mast test team in Control-Structures Interaction.

References

[1]Juang, J. N., and Pappa, R. S., "An Eigensystem Realization Algorithm (ERA) for Modal Parameter Identification and Model Reduction," *Journal of Guidance, Control, and Dynamics,* Vol. 8, No. 5, 1985, pp. 620–627.

[2]Mook, D. J., and Junkins, J. L., "Minimum Model Error Estimation for Poorly Modeled Dynamic Systems," *Journal of Guidance, Control, and Dynamics,* Vol. 11, No. 3, 1988, pp. 256–261.

[3]Mook, D. J., and Lew, J. S., "A Robust Algorithm for System Realization/Identification," *Journal of the Astronautical Sciences,* Vol. 38, No. 2, 1990, pp. 229–243.

[4]Roemer, M. J., and Mook, D. J., "Enhanced Realization/Identification of Physical Modes," *ASCE Journal of Aerospace Engineering,* Vol. 3, No. 2, 1990, pp. 122–136.

[5]Roemer, M. J., and Mook, D. J., "An Enhanced Mode Shape Identification Algorithm," *Proceedings of the 30th AIAA/ASME/ASCE/AHS Structures, Structural Dynamics, and Materials Conference,* AIAA, Washington, DC, 1989.

[6]Roemer, M. J., and Mook, D. J., "Robust Realization/Identification of Damped Structures," AIAA Paper 89-1245, *Proceedings of the Damping 89 Conference,* West Palm Beach, FL, Feb. 1989.

[7]Mook, D. J., and Lin, J. C., "Minimum Model Error Estimation of Modal Truncation Errors," *Proceedings of the 1987 Spring Meeting of the Society for Experimental Mechanics,* Houston, TX, June 1987.

[8]Juang, J. N., and Pappa, R. S., "Effects of Noise on Modal Parameters Identified by the Eigensystem Realization Algorithm," *Journal of Guidance, Control, and Dynamics,* Vol. 9, No. 3, 1986, pp. 294–303.

[9]Mook, D. J., and Lew, J. S., "Multiple Shooting Algorithms for Jump Discontinuous Problems in Optimal Estimation and Control," *IEEE Transactions on Automatic Control,* Vol. 36, No. 8, 1991, pp. 979–983.

[10]Pappa, R., et al., "Mini-Mast CSI Testbed Users Guide," NASA Langley Research Center, Hampton, VA.